Automation in Construction 95 (2018) 98–106

Contents lists available at ScienceDirect

Automation in Construction

journal homepage: www.elsevier.com/locate/autcon

Large-scale 3D printing by a team of mobile robots

Xu Zhang, Mingyang Li, Jian Hui Lim, Yiwei Weng, Yi Wei Daniel Tay, Hung Pham, Quang-Cuong Pham*

Singapore Centre for 3D Printing, School of Mechanical & Aerospace Engineering, Nanyang Technological University, 50 Nanyang Avenue, 639798, Singapore

ARTICLE INFO

Keywords:
3D cementitious material printing
Additive manufacturing
Building and construction
Multi-robot
Large-scale 3D printing

ABSTRACT

Scalability is a problem common to most existing 3D printing processes, where the size of the design is strictly constrained by the chamber volume of the 3D printer. This issue is more pronounced in the building and construction industry, where it is impractical to have printers that are larger than actual buildings. One workaround consists in printing smaller pieces, which can then be assembled on-site. This workaround generates however additional design and process complexities, as well as creates potential weaknesses at the assembly interfaces. In this paper, we propose a 3D printing system that employs multiple mobile robots printing concurrently a large, single-piece, structure. We present our system in detail, and report simulation and experimental results. To our knowledge, this is the first physical demonstration of large-scale, concurrent, 3D printing of a concrete structure by multiple mobile robots.

1. Introduction

Compared to traditional construction techniques, 3D-printing (also known as Additive Manufacturing) carries the promise of faster, safer, more customizable, and less labour-intensive operations in multiple segments of the Building and Construction (B&C) industry [1]. Recent years have seen rapid developments in 3D-printing for B&C, from the formulation of printable materials [2–4], to the design of new printing systems [5–9], to commercialization [10,11].

A major hurdle to the widespread adoption of 3D-printing in B&C is the limitation on the sizes of the printed structures. As reviewed in detail in Section 2, most existing 3D-printing systems for B&C are based on a gantry, which can only print structures whose sizes are at most as large as that of the gantry itself. Some arm-based systems have been demonstrated, but the sizes of the printed structures in this case are limited by the reach of the robotic arm. One workaround consists in printing smaller pieces, which can then be assembled together. This workaround generates however additional design and process complexities, as well as creates potential weaknesses at the assembly interfaces.

To overcome this scalability issue, we propose in this paper a 3D-printing system based on a team of multiple mobile robots. Such a system can potentially print single-piece structures of arbitrary sizes, depending on the number of deployed robots. We demonstrate, for the first time to our knowledge, the actual printing of a single-piece concrete structure by two mobile robots operating concurrently (see Fig. 1 and video at https://youtu.be/p_jcG25tUoo). The size of structure is 1.86 m × 0.46 m × 0.13 m (length, width, height), which is larger than the reach of each robot arm taken separately (1.74 m), highlighting the need for multi-robot deployment. According to the classification method proposed in [12], where concrete 3D-printing techniques are classified based on object scale (x_o), extrusion scale (x_e), environment (e), assembly strategies (a) and support (s), our system of collaborative printing is categorized as $x_o^1 x_e^1 e^0 a^0 s^0$ with robotic complexity of r_6, which is higher than all state-of-the-art techniques as recorded in [12]. Note that concurrent printing is important to guarantee good bonding properties at the junctions: sequential printing would lead to fresh concrete adjoining hardened concrete at the junctions, weakening thereby the bonding strength [3,13].

Concurrent 3D printing by multiple mobile robots is difficult for several reasons. First, the robot motions must be carefully planned and coordinated to optimize material delivery while avoiding mutual collisions. Second, robot localization must be highly precise to ensure that the pieces printed by different robots are perfectly aligned. Finally, the mixing and pumping systems of the robots must be coordinated to deliver materials in a synchronized manner.

The remainder of the article is organized as follows. In Section 2, we review existing 3D-printing systems for B&C. In Section 3, we present in detail our system based on a team of mobile robots. In Section 4, we report the results of the multi-robot printing experiment. In Section 5, we discuss the advantages and limitations of the proposed system. Finally, in Section 5.1, we conclude and sketch some directions for future

* Corresponding author.
E-mail address: cuong@ntu.edu.sg (Q.-C. Pham).

https://doi.org/10.1016/j.autcon.2018.08.004
Received 29 April 2018; Received in revised form 20 July 2018; Accepted 10 August 2018
Available online 16 August 2018
0926-5805/ © 2018 Elsevier B.V. All rights reserved.

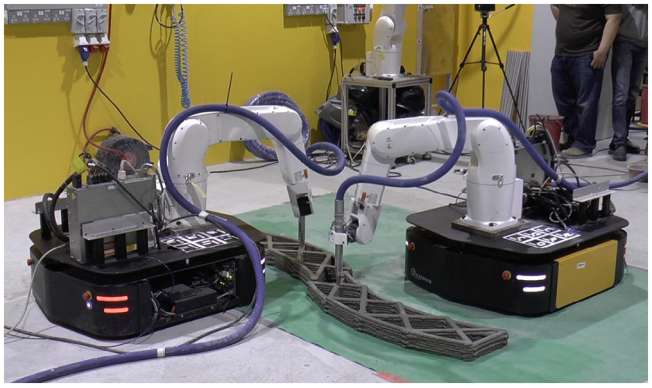

Fig. 1. Concurrent printing of a large, single-piece, concrete structure by two mobile robot printers. See the full video of the experiment at https://youtu.be/p_jcG25tUoo.

work.

2. Related works

2.1. Material development of 3D cementitious material printing

In recent years, various 3D concrete printing materials have been developed, categorized primarily into 3D printable plain concrete [2,3,14], 3D printable geopolymer [15], 3D printable fibre reinforcement concrete [16,17], 3D printable rapid hardening materials [18,19] and 3D printable earth-based materials [20]. These materials share a common emphasis on their rheological performances, which directly impacts the buildability and printability of 3D concrete printers, quantified by measurements such as printed height and pumping pressure respectively.

In the literature, several material models have been developed to understand material behaviour. Perrot et al. first established a model correlating yield stress and geometric factor to buildability [21], and his study was extended by Weng et al. towards more realistic application [22]. Weng's built-up model predicts the buildability of hollow cylinder using material static yield stress and geometric factor of the printing design. Wolfs et al. have shown that the elastic properties evolution is also critical in order to avoid structure collapse by buckling [23]. In another rheology study, Chhabra et al. proposed a model relating pumping pressure to rheological performance [24]. His model indicates that pumping pressure is governed by material plastic viscosity. Concrete is thixotropic [25] due to its continuous hydration, and this mean that its viscosity becomes less viscous when undergoing shear stress due to pumping. From these earlier works done, it is clear that the rheological property and elastic properties evolution of concrete are essential factors affecting concrete printing in terms of buildability and pumpability.

2.2. 3D concrete printing systems

Concrete printing systems can be divided based on their system mechanism, which is primarily gantry systems and robotic arm systems.

2.2.1. Gantry-based systems

The gantry system is widely adopted and uses a gantry to position the print nozzle in XYZ Cartesian coordinates. The build envelope of the gantry system is determined by enclosed volume of the gantry. A number of notable gantry systems include Contour Crafting [5,26–28], Concrete Printing [2,29,30] and D-shape [6].

These three techniques differ in their printing technique, with Contour Crafting and Concrete printing using an extrusion-based method similar to the Fused Deposition Method in additive manufacturing, and D-shape uses a binder jetting technique to selectively deposit binders on a powder bed made up of magnesium-based materials and sand. Another difference between Contour Crafting and Concrete printing is Concrete Printing's use of printing supports, which allows Concrete Printing to print full 3D topology as compared to Contour Crafting's vertical extrusion of a planar shape.

2.2.2. Arm-based systems

Robotic arm systems are relatively new compared to the gantry system counterparts. They provide additional roll, pitch and yaw controls to the end effector (print nozzle), allowing the print nozzle to perform more articulate print designs, such as printing with the tangential continuity method [7]. The tangential continuity method allows a smoother transition between print layers by maintaining a continuous rate of curvature change, giving a more aesthetically pleasing look. Another robotic arm system by Keating et al. [8] in Digital Construction Platform (DCP), they mounted the robotic arm on a track driven mobile platform for on-site fabrication of printed structures. DCP's system is also self-sufficient by recharging its electrical drive system with solar panels. One other mounted robotic arm system is Cybe RC 3Dp [31] which has a 6-axis robotic arm mounted on caterpillar tracks and is used in 3D printing the R&Drone Laboratory in Dubai [11].

2.2.3. Minibuilders

Minibuilders [9] presents an alternative approach for 3D concrete printing. They use three small mobile robots in the system. The first robot is equipped with a sensor that follows an initial marked path and builds the concrete foundation. The second robot is placed on the foundation and gripped the foundation with rollers before printing additional layers of concrete, and building up the structure. The last robot uses suction cups and pressurized air to print vertically up the printed structure and reinforced the printed structure which had only horizontal layers.

2.2.4. Summary

The biggest limitation in literature of printing system is their lack of scalability. Gantry-based system and stationary robotic arm system requires a massive external framework to support the single print nozzle in building the structure. While mobile robotic arm system helps extend the printing range, a single print nozzle still hoards the entire print space, limiting the efficiency of the printer. Although a multiple agent system is introduced by Minibuilders, their robots requires a harden structure for climbing and therefore has limited application as it involve waiting for the printed concrete to grant sufficient strength before deployment.

This gap in scalability motivates our project of a multi-robot printing system. Our system utilizes multiple mobile robot printers in a multi-agent setting to print their individual portion of a large print structure. They are capable of localization, collision avoidance and efficient coordinated printing through optimal robot placement. Our system demonstrate scalability by allowing users to introduces as many robots as needed in a shared environment for task completion in a fast and efficient manner.

2.3. Robotics background

Some robotics knowledge of the algorithms used in our proposed system for robot localization and planning is introduced in this section.

2.3.1. Simultaneous localization and mapping (SLAM)

Self-localization is critical for mobile robots to allow it to navigate its environment. The common strategy for localization in an unstructured environment involves using Simultaneous localization and mapping (SLAM) to construct and or update the map of the environment while keeping track of the robot in the environment [32–34]. A recent literature survey on state-of-the-art methodologies for

implementing solutions to the SLAM problem can be found in [35].

2.3.2. Motion planning

A fundamental motion planning task is to plan collision-free motions for a robot to move from a start to a goal position among a collection of obstacles [36]. The problem is often solved in configuration space, which is the set of all possible configurations for the robot.

Low-dimensional problems can be generally solved using grid-based algorithms that overlay a grid on top of configuration space and map each configuration to a grid point, or geometric algorithms where shape and connectivity of free space are computed. However, sampling-based algorithms are commonly used for high-dimensional problems due to their higher computational efficiency, where configuration space is represented with a road map of sampled configurations.

When it comes to path planning for multiple robots, there are basically two approaches: coupled and decoupled. A coupled planner treats the robots as a single combined robot and computes a path in a combined configuration space.

3. Large-scale 3D printing by multiple mobile robots

3.1. System setup

Each mobile robot printer in our setup consists of a holonomic mobile platform, a 6-axis robotic arm, a stereo camera and a pump as shown in Fig. 2. The robotic arm is mounted on the holonomic mobile platform and is equipped with a print nozzle. The robotic arm has a reach of 0.9 m with a repeatability of 0.02 mm. The holonomic mobile platform is equipped with sensors for localization and odometry, which includes wheel encoders, inertial measurement unit (IMU) and a 2D laser scanner. Localization is performed using on-board sensors, the stereo camera and some ArUco markers [37] placed on the platform. The markers have a black border for fast tracking and an inner binary matrix which determines its identifier, preventing feature mismatch. The pump system is responsible for delivering cementitious material to the print nozzle for selectively concrete deposition to build up the final print structure.

3.2. Pipeline

The printing pipeline is illustrated in Fig. 3.

Firstly, for a given 3D CAD model, it was sliced into thin, closely packed paths in a layer wise fashion. The coordinates and normal of the path were extracted as way points for the robotic arm. Using the geometry information of each layer, the multi-robot placement situation was formulated as an optimization problem, which was solved for finding feasible and reasonable pose for each corresponding robotic manipulator. A feasible solution is defined if a robot is its placement can deposit material accurately onto the desired print path without self-collision or exceeding its joint limit, while a reasonable solution is defined if the robot is able to avoid potential failure points if there is a better solution. The algorithm for multi-robot placement optimization will be illustrated in Section 3.4.

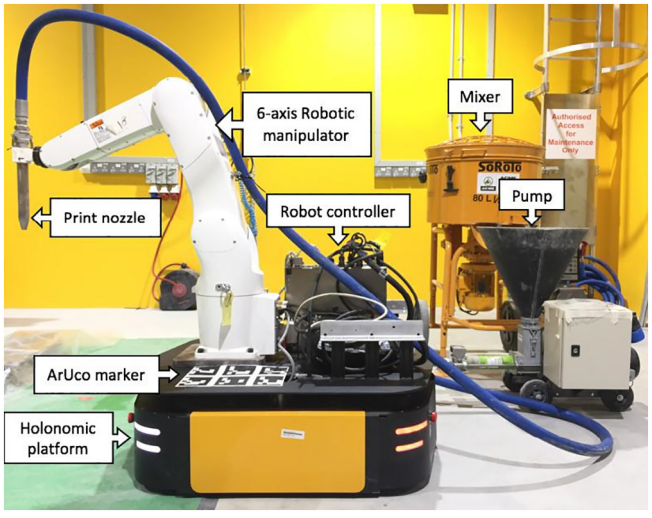

Fig. 2. System setup for one robot printer (stereo camera is placed out of the scene).

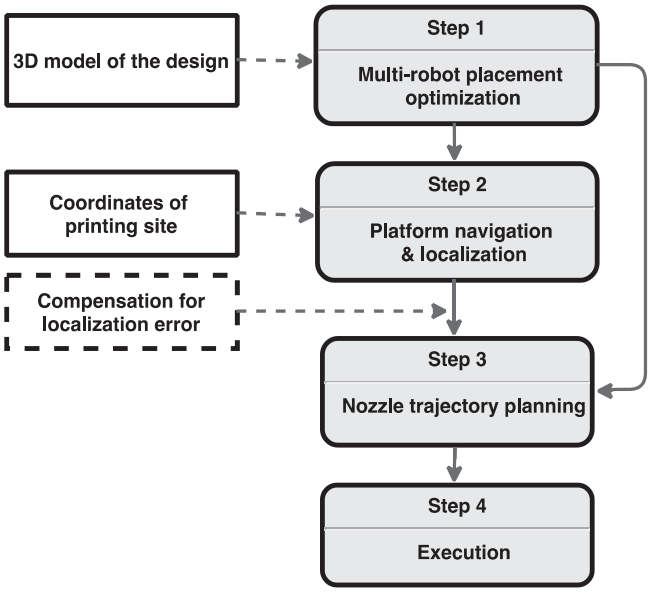

Fig. 3. Printing pipeline.

Secondly, with the construction environment and robot placement, the mobile robots would navigate to their respective target position accurately and without collision. In this phase, an environment map is generated with the on-board sensors and feasible paths are planned for navigation. When the mobile robots are in proximity to their target position, they are guided to their final position, using the stereo cameras. This methodology will be explained in Section 3.5.

Subsequently, the nozzle trajectory is planned so that it can extrude cementitious material accurately onto the required path in a time-coordinated manner in order to avoid collision with the environment, the printed structure and the other robot printers. This trajectory planning phase is done in parallel while the robot printer is navigating its environment. The nozzle trajectory planner takes into account the individual sub-workspace of each robot and the coordinates and normal of the way points generated in the first module, while correcting for minor error in the mobile platform localization. The algorithm for the multi-robot motion will be discussed in Section 3.6.

Finally, with the robot printers in their respective position, the printing process will begin.

3.3. Materials preparation and extrusion methods

The cementitious materials were designed to meet rheological requirements (yield stress and viscosity) for printing, and this was reflected by pumpability during the material delivery phase and buildability during the extrusion phase. Two separate materials were chosen to demonstrate the adaptability of the system towards multi-material printing. One material consists of ordinary concrete with its mix design shown in Table 1, and the other material is a fibre reinforced concrete mix design [22] and shown in Table 2.

Two SoRoTo Forced Action Mixer 80 L were used in mixing. As mixing factors, such as mixing time, speed and temperature, have been known to affect cementitious material rheological properties, mixing

Table 1
Mixture proportion for robot printer 1 (kg/m^3).

Materials	Cement	Fly ash	Silica fume	River Sand	Water
	(OPC, ASTM Type 1)	(Class F)	(Undensified, Elkem)		
Proportion	613.7	287.7	57.5	767.2	402.8

Table 2
Mixture proportion for robot printer 2 (kg/m^3).

Materials	OPC	Sand	Water	Fly ash	Silica fume	Superplasticizer
Proportion	575.7	590	330.3	575.7	863.4	1.4

Note: All ingredients contents are expressed as weight proportion of cement content.

procedures were strictly standardised and adhered to, so as to ensure the consistency of rheology performance. Firstly, the powder of all solid ingredients was dry mixed for 1 min at stir speed; water was then added and mixed for another minute at stir speed. Superplasticizer was added, and the mixing speed was increased to speed I for 1 min, and speed II for 1 min. Finally, the fibre is introduced, and the mixing process continued for 2 min at speed II. On completion of the mixing procedures, the cementitious material was loaded into the pumps' hoppers.

During printing, a rotor/stator pump was used to deliver the cementitious material through a 5 m long 25.4 mm diameter hose pipe at 650 rpm. The cementitious material was extruded through a 10 mm tapered diameter print nozzle to build up the designed structure in a layer wise manner. The choice of a round nozzle also eases the orientation constraint on the nozzle allowing a wider pose solution to be found, which translates to a bigger printing volume by the robot printer.

3.4. Robot placement optimization

In literature, there are multiple studies on collision avoidance for multiple robots working in a shared workspace [38–40] or optimal robot placement given a prescribed task [41,42] but not the combination of two situations which is required in our multi-robot printing system. The multiple robotic printers have to cover the complete work piece in a collision-free environment yet no overlap of their individual workspace is allowed. We previously formulated this situation as an optimization problem that tries to minimize the length of work piece that is not able to be covered.

However, just satisfying workspace coverage might result in some robot configurations that would cause potential planning problems. In this work, we further improve the algorithm by introducing a score scheme for robot configuration considering its kinematic reachability.

The kinematic reachability of a point in the robot workspace is given by the number of possible robot configurations which realize this point. A kinematic reachability database for one robot printer was generated prior to printing (See Fig. 4).

Kinematic reachability was then normalized to the interval from 0 to 1 and was incorporated to an optimization program to find the optimal robot placement. In general, let N denote the number of robot printers, the optimization objective function is given by

$$\underset{\boldsymbol{x}_1,\ldots,\boldsymbol{x}_N \epsilon SE(2)}{\operatorname{argmin}} \; -\sum_{i=1}^{N} \boldsymbol{S}(\boldsymbol{x}_i) + \boldsymbol{C}(\boldsymbol{x}_1,\ldots,\boldsymbol{x}_N) \tag{1}$$

where $\boldsymbol{x}_i$ is the pose of the i-th robot printer, $\boldsymbol{S}(\boldsymbol{x}_i)$ evaluates the total reachability of the i-th robot printer regarding the target object, $\boldsymbol{C}(\boldsymbol{x}_1, \ldots, \boldsymbol{x}_N)$ is the cost of collision between the robots, which is assigned to 0 if the system is collision-free and a large value if collisions exist.

3.5. Robot localization

Among the myriad of SLAM algorithms, we have adopted GMapping [43] for map construction because of its high efficiency and accuracy. Fig. 5(a) shows a map of our lab constructed with the sensors on board of the platform using GMapping. The constructed map was then used in adaptive Monte Carlo localization (AMCL) [44] for robot localization.

In Fig. 5(b) the rainbow colour thin lines were from the sensor data, while the blue regions are places considered occupied on the occupancy grid map. It showed the situation that the mobile robot succeeded in localizing itself in the map using AMCL algorithm, with the sensor observations fitting the given map well.

With the SLAM and AMCL algorithms, mobile platforms are able to localize themselves in a rough-scale and navigate in the environment at a low cost. However, this is far from the precision required for them to print concurrently on one work piece. Hence, we switched to vision control when the platform is near to the target printing site for higher accuracy. ArUco markers were attached on the mobile platforms and stereo cameras were installed around the construction site, providing easy and unique features for the camera to identify and avoid feature mislabels when using nature features in the environment. Upon observation of the markers, relative pose between the camera and the detected marker is calculated, and the robot can localize its position unambiguously.

3.6. Multi-robot motion planning

Motion planning is required for robot navigation and nozzle trajectory planning for multiple robot printers. In this work, we use decoupled planning approach since it is generally faster. Before talking about planning algorithms, it would be helpful to know that in the syntax of robotics, trajectory is a time-parametrized path, which indicates how fast a path is executed. We first compute a path for each robot independently, then use a coordination diagram to plan collision-free trajectories for each robot along its path. The second step can be thought of as a re-timing process, which is analogical to finding a path from (0, 0, …, 0) to (l_1, l_2, …, l_n) of a virtual cube with perpendicular axes representing trajectories of the robots. Each point inside the cube corresponds to one combination of robot configurations at particular time instance.

The above stated trajectory planning is a naive process which assumes perfect execution of the trajectory. However, for platform navigation the uncertainty can be significant due to the slippery of the wheels and imperfect condition of the floor, especially for construction environment. Therefore, to avoid collision of the mobile platforms and to navigate to the goal positions accurately, the platforms broadcast their locations at certain frequency for collision checking, and the trajectory is re-planned upon update of new data.

3.7. Actual printing

We used Ubuntu operating system for system integration [45], ROS for device control, message-passing between processes and package management [46], and OpenRAVE for planning and collision checking.

Prior to printing, a kinematic reachability database of the robot printers was generated. Subsequently, a map of the printing site was constructed with GMapping by moving a robot printer around the printing site. Stereo cameras were also set up around the site.

By slicing a 3D model of the target object, the waypoints, each consists of XYZ coordinates and a normal vector, were generated. This can be carried out using common slicing programs for 3D printing.

Next, taking as inputs the target printing pattern, the robot printers' models and their kinematic reachability databases, the algorithm in Section 3.4 was used to compute the desired placement of the robot printers.

Subsequent to robot placement optimization, trajectories for the

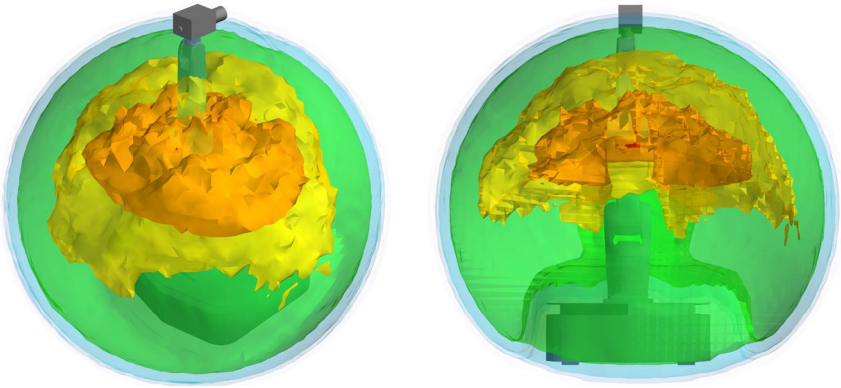

(a) Isometric view (b) View along the x

Fig. 4. Kinematic Reachability of a robot printer. The colours represent different levels of kinematic reachability: green and orange denoting the highest and lowest levels respectively. (For interpretation of the references to colour in this figure legend, the reader is referred to the web version of this article.)

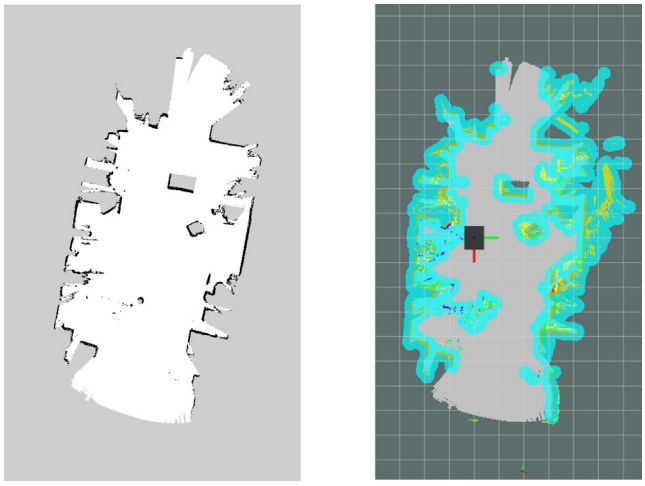

(a) Map of the printing site constructed by GMapping. (b) Robot printer localization in the map achieved by AMCL

Fig. 5. Map construction and robot printer localization.

print nozzles are planned in OpenRAVE so that they can deliver material accurately on the desired paths without causing collisions with printed parts and other robot printers. Concurrently, the mobile printers plan their trajectories from home station to target printing positions using the map of the printing site constructed in earlier stage.

Upon completion of the planning, mobile printers navigate towards their target printing locations, using AMCL algorithm to track the mobile printers. In an effort to increase the robot localization accuracy, when the printers are within a pre-defined proximity to their target position, they will switch to vision-feedback control using the stereo cameras to track the ArUco markers placed on the mobile platforms. On reaching their target locations, the printers start to print on the work piece concurrently following the planned paths. The planned paths may be re-planned at this stage to compensate for any minor error in platform localization as discussed in Section 3.2.

Upon completion of printing, the robot printers will return to their home station, using the same navigation strategies when moving to the printing location. In the entire process, the robot printers will broadcast their status for collision checking, and also to synchronize the printing with the pumping system.

4. Results

Results of both simulation and demonstration on actual robotic system are presented in this section.

4.1. Simulation

In the simulation as shown in Fig. 6, two robot printers were required to build a large-scale structure whose size is beyond the printing volume of one single robot printer.

It took 24 s to plan for mobile platform navigation from home station to target printing locations, and 25 s from printing location back to home station. Planning of trajectories for the print nozzles to print 12 layers of the target structure took 11 s.

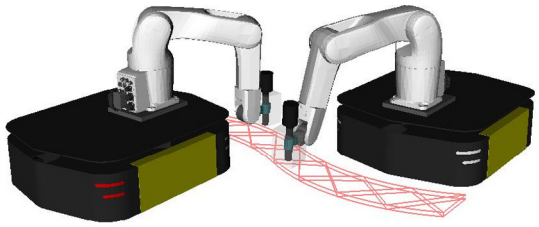

(a) Concurrent printing of one large-scale structure by two mobile robot printers.

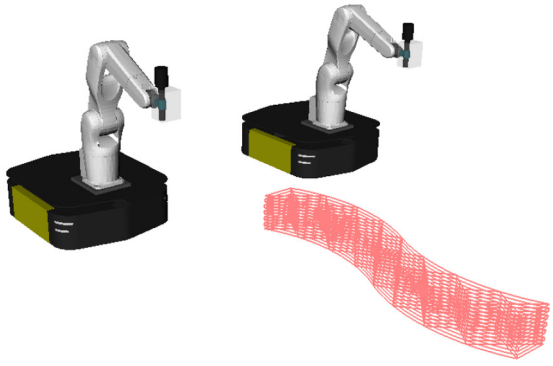

(b) Robot printers back to home station upon completion of printing.

Fig. 6. Simulation of multi-robot printing process.

4.2. Execution

The simulation in Section 4.1 has been implemented on actual robotic system with the proposed printing pipeline. Fig. 7 presents an ordered sequence of intermediate steps during the printing process.[1]

Given target printing location and printing pattern, placement of robot printers and their corresponding printing paths were simulated. The two robot printers navigated from home station to their respective printing locations. Subsequently they started printing concurrently on the large structure in a coordinated fashion without collision. Upon completion of the print, the robot printers return to the home station.

4.3. Printed specimen

The printed structure was 1.86 m × 0.46 m × 0.13 m (length, width, height). The specimen was covered by a plastic sheet to simulate field conditions for ambient curing. After 10 days of curing, we could turn it over, as shown in Fig. 8.

The mechanical properties of the 3D printed concrete with each of the two materials can be found in [4,22]. Regarding the junctions, we did not perform tests (since this would involve cutting the specimen), but noted that the bonding strength was high enough to easily support the specimen's own weight when it was placed on its side (Fig. 8(b)). Informal visual and stress inspections suggested that the bonding was strong. Extensive and quantitative tests will be performed as part of our future work.

5. Discussion

The printing demonstration in Section 4.2 serves as a proof of concept for the multiple mobile robots printing system for printing concrete structure in an efficient and scalable manner. The printed design was chosen to incorporate complex curves and internal void that would be challenging to build using traditional construction methods. The size of the printed design was also chosen to extend beyond the workspace of a single robot printer, requiring the concurrent printing by multiple robots. With the decoupling of printer system from print material, it allows flexibility for users in selection of materials for different applications such as printing a load bearing structural wall to wall fillers. Our demonstration has intentionally used two different materials in showing its non-reliance on material type, as mentioned in Section 3.3.

As our proposed system has the attribute of arm-based system, mobile platform and swarm printing, its major advantages over gantry-based system, stationary printer and single printer are discussed here.

5.1. Advantages over gantry-based system

Robotic arm printers benefit from the greater flexibility of having full 6 degrees of freedom as compared to 3 or 4 degrees of freedom in the conventional gantry system.

This extra articulation allows the robotic arm printer to print complex curved parts using the tangential continuity method [7,47]. This results in a smoother transition between print layers by maintaining a continuous rate of curvature change, hence giving a structurally more efficient mechanical stability by reducing shear loads between printed layers.

5.2. Advantages over stationary printer

The mobile platform of our robot printer extends the reachability of the printer, by allowing the printer to print beyond the fixed environment it will otherwise be confined to when stationary. On-site robotic 3D printing is expected to alleviate transportation cost, as printing large structures on site helps to relieve pressure of transporting oversized parts that would not fit on a conventional truck.

5.3. Advantages over single printer

Swarm printing affords greater scalability and efficiency as compared to a single printer. It has been shown in our demonstration that swarm printer can build structure whose size (1.86 m × 0.46 m × 0.13 m) is larger than the reach of a single printer (1.74 m). When the same structure is to be printed with a single printer, it took twice the required duration of two printers.

However, there are also challenges for the system to work robustly for application in B&C industry. A major technical difficulty would be accurate localization of the robot printer under different terrain conditions. When the terrain is bumpy and dusty, which is common to a construction site, the mobility scheme for the mobile printer plays a vital role in the printing system. As Mecanum wheel designs for holonomic mobiles can perform poorly on rough terrains [48], it would be necessary to investigate alternative wheel schemes to enhance the robustness of the printing, such as differential tank drive.

6. Conclusion and future works

6.1. Conclusion

In this paper, we have demonstrated a multi-robot printing system that is capable of on-site printing large structures in a safe, efficient and scalable manner. The system configuration contains several modules: planning of robot placement to optimize workspace, mobile robot navigation and localization to reach target printing location, and planning of manipulator trajectory to deposit material accurately on desired path.

We presented our results of both simulation and demonstration on actual robotic system: two mobile robot printers work concurrently on one structure whose size is twice the printing volume of one single printer.

Comparing to existing 3D cementitious material printing techniques, experimental results suggest that the proposed system is superior in its greater practical scalability and higher time efficiency due to the employment of multiple robot printers, as well as better on-site printing capability credited with mobility of the system. These advantages make the proposed system promising to be scaled up for on-site large-scale printing applications in B&C industry. Both technical and economic benefits can be evaluated by the Construction Robotic Equipment Management System (CREMS) [49–52]. Furthermore, using a fleet of mobile robots for construction could have an extreme potential in other non-conventional aspects. One such application is to allow automated construction in hard-to-reach, remote areas, such as underground caves, the Moon or Mars [53], to which it is inconvenient or even impossible to bring other kinds of machine required for existing cementitious material printing methods.

A technical concern of the proposed system is the complexity in coordinating such a fleet of mobile robots. However, this paper demonstrates that this difficulty can be significantly mitigated by utilizing standard robotic techniques.

6.2. Future works

With our successful proof-of-concept demonstration of the proposed multi-robot printing system, our primary future plan is to integrate the overall system to boost automation to a greater extent.

Moving forward from current printing-on-arrival scheme, where robot printers navigate towards desired printing locations and start to print at these stationary locations, our future research direction will

[1] Timings taken from the Supplement video material: 10 s to move to printing position, 470 s for printing (7 min 50 s), 10 s to move back to home station.

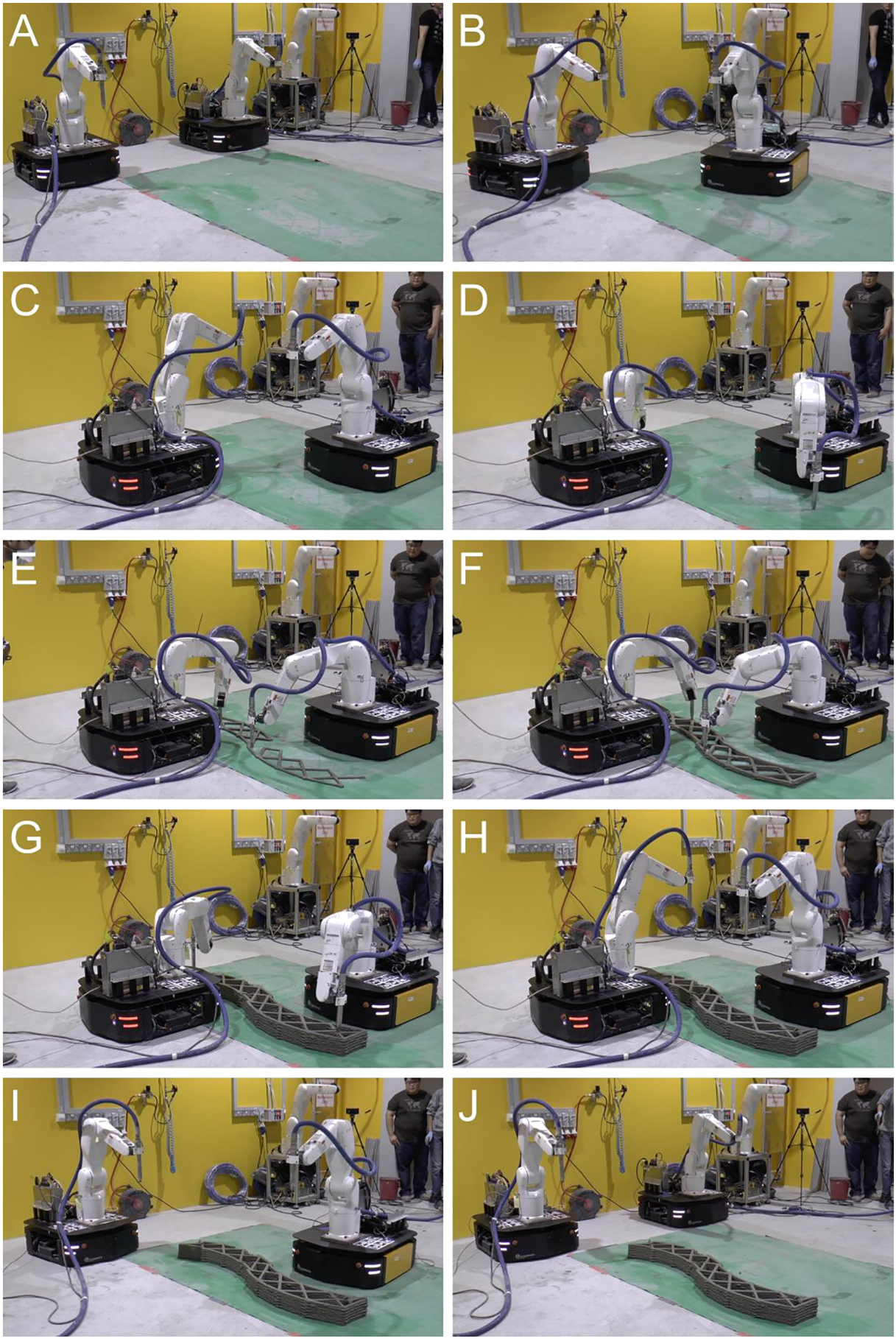

(caption on next page)

Fig. 7. Snapshots taken during the actual printing process. See the full video of the experiment at https://youtu.be/p_jcG25tUoo. A. Robot printers at home station; B. Navigating towards target locations; C. Reaching target locations; D. Starting printing; E. Printing in progress; F. Building up layers; G. Finishing printing; H. Robotic manipulators back to standby pose; I. Navigating back; J. Reaching home station.

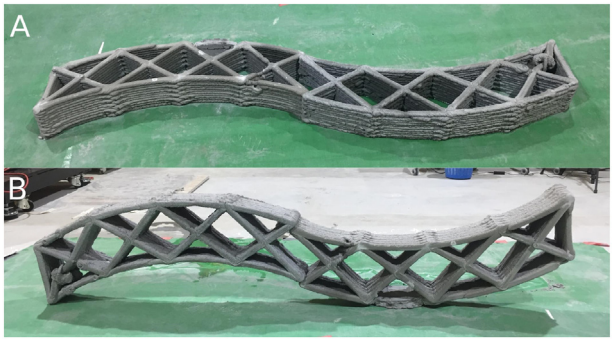

Fig. 8. Printed specimen after 10 days of curing.

focus on study of printing-while-moving scheme to fully utilize the advantage of mobile robot printer and further extend the printing scale. On account of the integration of printing-on-arrival and printing-while-moving, the study will also involve investigation of trade-off between workspace size covered by each single mobile robot printer and inter-layer strength of 3D printed concrete.

Apart from exploring alternative wheel schemes, future work would include integration of additional sensors that aids in the online determination of nozzle offset distance to compensate for changes in ground level while printing.

In addition, bonding strategies at the interface of two separate concrete prints would be carried out to identify the optimal method of joining, which could be face-to-face joint or finger joints. Such methods would seek to reduce the degree of material overlapping that could adversely affect part appearance while maximising interface area for stronger bond.

Supplementary data to this article can be found online at https://doi.org/10.1016/j.autcon.2018.08.004.

Acknowledgement

This research is supported by the National Research Foundation, Prime Ministrer's Office, Singapore under its Medium-Sized Centre funding scheme, Singapore Centre for 3D Printing, and Sembcorp Design & Construction Pte Ltd. The authors would like to thank Y. Qian, B. Panda, W. Lao, Z. Liu, A. Ting, and A. Annapareddy for their helps with the experiment, Prof. S. Qian and Prof. M. Tan for helpful discussions.

References

[1] Y.W.D. Tay, B. Panda, S.C. Paul, N.A. Noor Mohamed, M.J. Tan, K.F. Leong, 3D printing trends in building and construction industry: a review, Virtual Phys. Prototyp. 12 (3) (2017) 261–276, https://doi.org/10.1080/17452759.2017.1326724.

[2] T.T. Le, S.A. Austin, S. Lim, R.A. Buswell, R. Law, A.G. Gibb, T. Thorpe, Hardened properties of high-performance printing concrete, Cem. Concr. Res. 42 (3) (2012) 558–566, https://doi.org/10.1016/j.cemconres.2011.12.003.

[3] B. Zareiyan, B. Khoshnevis, Interlayer adhesion and strength of structures in contour crafting-effects of aggregate size, extrusion rate, and layer thickness, Autom. Constr. 81 (2017) 112–121, https://doi.org/10.1016/j.autcon.2017.06.013.

[4] Y.W. Tay, B. Panda, S.C. Paul, M.J. Tan, S.Z. Qian, K.F. Leong, C.K. Chua, Processing and properties of construction materials for 3D printing, Mater. Sci. Forum 861 (2016) 177–181, https://doi.org/10.4028/www.scientific.net/MSF.861.177.

[5] B. Khoshnevis, R. Dutton, Innovative rapid prototyping process makes large sized, smooth surfaced complex shapes in a wide variety of materials, Mater. Technol. 13 (2) (1998) 53–56, https://doi.org/10.1080/10667857.1998.11752766.

[6] G. Cesaretti, E. Dini, X. De Kestelier, V. Colla, L. Pambaguian, Building components for an outpost on the lunar soil by means of a novel 3D printing technology, Acta Astronaut. 93 (2014) 430–450, https://doi.org/10.1016/j.actaastro.2013.07.034.

[7] C. Gosselin, R. Duballet, P. Roux, N. Gaudilliere, J. Dirrenberger, P. Morel, Large-scale 3D printing of ultra-high performance concrete–a new processing route for architects and builders, Mater. Des. 100 (2016) 102–109, https://doi.org/10.1016/j.matdes.2016.03.097.

[8] S.J. Keating, J.C. Leland, L. Cai, N. Oxman, Toward site-specific and self-sufficient robotic fabrication on architectural scales, Science Robotics 2 (5) (2017) eaam8986, , https://doi.org/10.1126/scirobotics.aam8986.

[9] IAAC, Minibuilders, http://robots.iaac.net , Accessed date: 29 June 2018.

[10] T.C. Nguyen, Yes, that 3D-printed mansion is safe to live in, https://www.washingtonpost.com/news/innovations/wp/2015/02/05/yes-that-3d-printed-mansion-is-safe-to-live-in/?utm_term=.2112831042ec , Accessed date: 29 June 2018.

[11] S. Saunders, CyBe construction announces that 3D printing is complete for Dubai's R &Drone Laboratory, https://3dprint.com/176561/cybe-3d-printed-dubai-laboratory/ , Accessed date: 29 June 2018.

[12] R. Duballet, O. Baverel, J. Dirrenberger, Classification of building systems for concrete 3D printing, Autom. Constr. 83 (2017) 247–258, https://doi.org/10.1016/j.autcon.2017.08.018.

[13] J.G. Sanjayan, B. Nematollahi, M. Xia, T. Marchment, Effect of sur-face moisture on inter-layer strength of 3D printed concrete, Constr. Build. Mater. 172 (2018) 468–475, https://doi.org/10.1016/j. conbuildmat.2018.03.232.

[14] S.C. Paul, Y.W.D. Tay, B. Panda, M.J. Tan, Fresh and hardened properties of 3D printable cementitious materials for building and construction, Arch. Civ. Mech. Eng. 18 (1) (2018) 311–319, https://doi.org/10.1016/j.acme.2017.02.008.

[15] B. Panda, S.C. Paul, L.J. Hui, Y.W.D. Tay, M.J. Tan, Additive manufacturing of geopolymer for sustainable built environment, J. Clean. Prod. 167 (2017) 281–288, https://doi.org/10.1016/j.jclepro. 2017.08.165.

[16] B. Panda, S.C. Paul, M.J. Tan, Anisotropic mechanical performance of 3D printed fiber reinforced sustainable construction material, Mater. Lett. 209 (2017) 146–149, https://doi.org/10.1016/j.matlet.2017.07.123.

[17] M. Hambach, D. Volkmer, Properties of 3D-printed fiber-reinforced Portland cement paste, Cem. Concr. Compos. 79 (2017) 62–70, https://doi.org/10.1016/j.cemconcomp.2017.02.001.

[18] N. Khalil, G. Aouad, K. El Cheikh, S. Remond, Use of calcium sulfoaluminate cements for setting control of 3D-printing mortars, Constr. Build. Mater. 157 (2017) 382–391, https://doi.org/10.1016/j. conbuildmat.2017.09.109.

[19] P. Shakor, J. Sanjayan, A. Nazari, S. Nejadi, Modified 3D printed powder to cement-based material and mechanical properties of cement scaffold used in 3D printing, Constr. Build. Mater. 138 (2017) 398–409, https://doi.org/10.1016/j.conbuildmat.2017.02.037.

[20] A. Perrot, D. Rangeard, E. Courteille, 3D printing of earth-based materials: processing aspects, Constr. Build. Mater. 172 (2018) 670–676, https://doi.org/10.1016/j.conbuildmat.2018.04.017.

[21] A. Perrot, D. Rangeard, A. Pierre, Structural built-up of cement-based materials used for 3D-printing extrusion techniques, Mater. Struct. 49 (4) (2016) 1213–1220, https://doi.org/10.1617/s11527-015-0571-0.

[22] Y. Weng, M. Li, M.J. Tan, S. Qian, Design 3D printing cementitious materials via Fuller Thompson theory and Marson-Percy model, Constr. Build. Mater. 163 (2018) 600–610, https://doi.org/10.1016/j. conbuildmat.2017.12.112.

[23] R. Wolfs, F. Bos, T. Salet, Early age mechanical behaviour of 3D printed concrete: numerical modelling and experimental testing, Cem. Concr. Res. 106 (2018) 103–116, https://doi.org/10.1016/j.cemconres. 2018.02.001.

[24] R.P. Chhabra, J.F. Richardson, Non-Newtonian Flow and Applied Rheology: Engineering Applications, Butterworth-Heinemann, 978-0-7506-8532-0, 2011, https://doi.org/10.1016/B978-0-7506-8532-0.X0001-7.

[25] N. Roussel, A thixotropy model for fresh fluid concretes: theory, validation and applications, Cem. Concr. Res. 36 (10) (2006) 1797–1806, https://doi.org/10.1016/j.cemconres.2006.05.025.

[26] B. Khoshnevis, Automated construction by contour craftingrelated robotics and information technologies, Autom. Constr. 13 (1) (2004) 5–19, https://doi.org/10.1016/j.autcon.2003.08.012.

[27] B. Khoshnevis, G. Bekey, Automated construction using contour crafting–applications on earth and beyond, Nist Special Publication Sp, 2003, pp. 489–494, , https://doi.org/10.22260/ISARC2002/0076.

[28] B. Khoshnevis, D. Hwang, K.-T. Yao, Z. Yeh, Mega-scale fabrication by contour crafting, Int. J. Ind. Syst. Eng. 1 (3) (2006) 301–320, https://doi.org/10.1504/IJISE.2006.009791.

[29] T.T. Le, S.A. Austin, S. Lim, R.A. Buswell, A.G. Gibb, T. Thorpe, Mix design and fresh properties for high-performance printing concrete, Mater. Struct. 45 (8) (2012) 1221–1232, https://doi.org/10.1617/s11527-012-9828-z.

[30] S. Lim, R.A. Buswell, T.T. Le, S.A. Austin, A.G. Gibb, T. Thorpe, Developments in construction-scale additive manufacturing processes, Autom. Constr. 21 (2012) 262–268, https://doi.org/10.1016/j. autcon.2011.06.010.

[31] Cybe RC 3Dp, https://cybe.eu/3d-concrete-printers/#1520593810901-9a0ee625-b8d5 , Accessed date: 29 June 2018.

[32] T. Bailey, H. Durrant-Whyte, Simultaneous localization and mapping (SLAM): part II, IEEE Robot. Autom. Mag. 13 (3) (2006) 108–117, https://doi.org/10.1109/MRA.2006.1678144.

[33] M.G. Dissanayake, P. Newman, S. Clark, H.F. Durrant-Whyte, M. Csorba, A solution to the simultaneous localization and map building (SLAM) problem, IEEE Trans.

Robot. Autom. 17 (3) (2001) 229–241, https://doi.org/10.1109/70.938381.
[34] S. Thrun, Simultaneous localization and mapping, Robotics and Cognitive Approaches to Spatial Mapping, Springer, 978-3-540-75386-5, 2007, pp. 13–41, , https://doi.org/10.1007/978-3-540-75388-9_3.
[35] C. Cadena, L. Carlone, H. Carrillo, Y. Latif, D. Scaramuzza, J. Neira, I. Reid, J. Leonard, Past, present, and future of simultaneous localization and mapping: towards the robust-perception age, IEEE Trans. Robot. 32 (6) (2016) 13091332, https://doi.org/10.1109/TRO.2016.2624754.
[36] S.M. LaValle, Planning Algorithms, Cambridge University Press, 9780511546877, 2006, https://doi.org/10.1017/CBO9780511546877.
[37] S. Garrido-Jurado, R. Munñoz-Salinas, F.J. Madrid-Cuevas, M.J. Marın-Jimenez, Automatic generation and detection of highly reliable fiducial markers under occlusion, Pattern Recogn. 47 (6) (2014) 2280–2292, https://doi.org/10.1016/j.patcog.2014.01.005.
[38] Y. Zhou, H. Hu, Y. Liu, Z. Ding, Collision and deadlock avoidance in multirobot systems: a distributed approach, IEEE Trans. Syst. Man Cybern. Syst. 47 (7) (2017) 1712–1726, https://doi.org/10.1109/TSMC.2017.2670643.
[39] D. Claes, K. Tuyls, Multi robot collision avoidance in a shared workspace, Auton. Robot. (2018) 1–22, https://doi.org/10.1007/s10514-018-9726-5.
[40] E. Freund, H. Hoyer, Real-time pathfinding in multirobot systems including obstacle avoidance, Int. J. Robot. Res. 7 (1) (1988) 42–70, https://doi.org/10.1177/027836498800700104.
[41] D. Spensieri, J.S. Carlson, R. Bohlin, J. Kressin, J. Shi, Optimal robot placement for tasks execution, Procedia CIRP 44 (2016) 395–400, https://doi.org/10.1016/j.procir.2016.02.105.
[42] B. Kamrani, V. Berbyuk, D. Wappling, U. Stickelmann, X. Feng, Optimal robot placement using response surface method, Int. J. Adv. Manuf. Technol. 44 (1–2) (2009) 201–210, https://doi.org/10.1007/s00170-008-1824-7.
[43] G. Grisetti, C. Stachniss, W. Burgard, Improved techniques for grid mapping with rao-blackwellized particle filters, IEEE Trans. Robot. 23 (1) (2007) 34–46, https://doi.org/10.1109/TRO.2006.889486.
[44] D. Fox, S. Thrun, W. Burgard, F. Dellaert, Particle filters for mobile robot localization, Sequential Monte Carlo Methods in Practice, Springer, 2001, pp. 401–428, , https://doi.org/10.1007/978-1-4757-3437-9_19.
[45] Ubuntu, https://www.ubuntu.com , Accessed date: 29 June 2018.
[46] A. Koubaa, Robot Operating System (ROS), Springer, 0-470-23457-1, 2017, https://doi.org/10.1007/978-3-319-26054-9.
[47] P. Bosscher, R.L. Williams II, L.S. Bryson, D. Castro-Lacouture, Cable-suspended robotic contour crafting system, Autom. Constr. 17 (1) (2007) 45–55, https://doi.org/10.1016/j.autcon.2007.02.011.
[48] A. Ramirez-Serrano, R. Kuzyk, Modified mecanum wheels for traversing rough terrains, in: M. Bauer, J.L. Mauri, O. Dini (Eds.), The Sixth International Conference on Autonomic and Autonomous Systems, IEEE, Cancun, Mexico, 2010, pp. 97–103, , https://doi.org/10.1109/icas.2010.35.
[49] J.S. Russell, M.J. Skibniewski, J.A. Vanegas, Framework for construction robot fleet management system, J. Constr. Eng. Manag. 116 (3) (1990) 448–462, https://doi.org/10.1061/(ASCE)0733-9364(1990)116:3(448).
[50] M.J. Skibniewski, J.S. Russell, Construction robot fleet management system prototype, J. Comput. Civ. Eng. 5 (4) (1991) 444–463, https://doi.org/10.1061/(ASCE)0887-3801(1991)5:4(444).
[51] M.J. Skibniewski, R. Kunigahalli, J.S. Russell, Managing multiple construction robots with a computer, Autom. Constr. 2 (3) (1993) 199–216, https://doi.org/10.1016/0926-5805(93)90041-U.
[52] M.J. Skibniewski, K. Tamaki, Logistics support system for construction robotics implementation, J. Comput. Aided Civ. Infrastruct. Eng. 9 (1) (1994) 69–81, https://doi.org/10.1111/j.1467-8667.1994.tb00363.x.
[53] Nasa's centennial challenges: 3-D printed habitat challenge, https://www.nasa.gov/directorates/spacetech/centennial_challenges/3DPHab/index.html , Accessed date: 29 June 2018.